NUMERICAL SIMULATION OF FLOW DYNAMICS IN THE PERIODIC REGIME INSIDE AN IDEALIZED THERMOACOUSTIC ENGINE

MA[1,2] L., WEISMAN[1,2] C., BALTEAN-CARLES[1,2] D., DELBENDE[1,2] I., BAUWENS[3] L.
[1]UPMC, 4 Place de Jussieu–75005 Paris, France
[2]LIMSI-CNRS, BP133 – 91400 Orsay, France
[3]University of Calgary, T2N 1N4, Canada
E-mail: malin@ limsi.fr

Abstract: Flow dynamics in the stack and heat exchangers of a standing wave thermoacoustic engine are studied using 2D numerical simulations. The numerical approach is based on asymptotic coupling in the low Mach number limit, of a nonlinear dynamic model in the active cell with linear acoustics in the resonator. Computed results of the periodic regime are analyzed and exhibit two main features: instability and vortex dynamics.

1. Introduction

A simplified model of a loaded thermoacoustic engine consists of a long tube closed at one side and loaded at the other side, inside which the active cell is placed. The active cell comprises a stack of parallel plates placed between two heat exchangers. One heat exchanger is connected to a hot source and the other to a cold source. The combined effect of pressure fluctuations and oscillating heat exchange in the boundary layers on the stack plates provides a heat engine effect [1, 2, 3]. A multiple scale formulation allows for the global compressible flow problem to be reduced to a dynamically incompressible problem in the active cell, with boundary conditions obtained from linear acoustics in the resonator. The detail of this analysis can be found in [4, 5].
In the literature there are few studies dedicated to nonlinear hydrodynamics inside the active cell. The purpose of this paper is to show and analyse numerical results on flow dynamics in the periodic regime, such as instability and vortex dynamics. After a brief introduction of the model and the numerical method, the computed results of the periodic regime are presented and discussed in two steps: first, the influence of the load on the onset temperature and saturation is presented, validating the choice of the load value. Then, the flow patterns, temperature field and vorticity field are analysed and a possible mechanism of the observed instability is discussed qualitatively.

2. Numerical approach

2.1 Geometry and model

The geometry consist of a long resonator with length L_{res}, within which an active cell with characteristic stack length L_s is placed. The active cell consists of a stack of parallel plates and two heat exchangers (heater and cooler). The heater and the cooler are also made of parallel plates. We assume the vertical periodicity, so that the simulation can be reduced to a domain consisting of two half-plates and the space between them, and the corresponding fraction of the resonator cross-section. The active cell is small compared to resonator length, therefore two characteristic length scales are to be considered, L_{res} and L_s. The geometry of the entire resonator is shown in Fig. 1 (top). The resonator dead end is located at $\hat{x} = -l_L$, while the other end consist of a load modelled as a real impedance f at the fixed location

$\hat{x} = +\ell_R$, with $p(\ell_R, t) = fu(\ell_R, t)$. The active cell is considered as a discontinuity section positioned at $\hat{x} = 0$.
Turning to the stack scale, the geometry of the active cell is shown in Fig. 1 (bottom) and boundaries with the resonator are pushed to infinity. This represents the simulation domain. In our case, the length is $5L_s$ and the height is H .

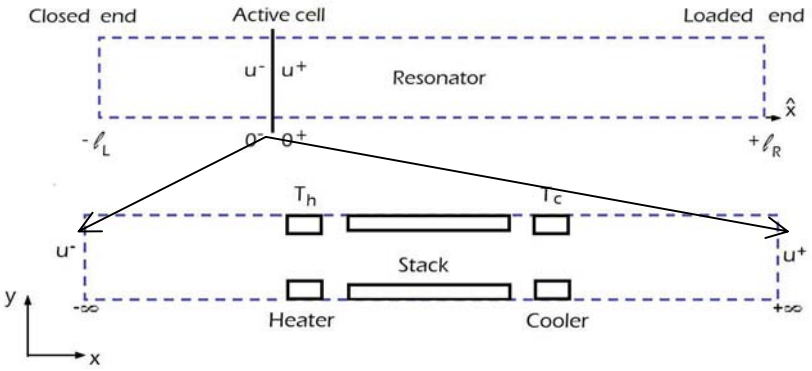

Figure 1: Geometry of linear acoustic system (top) and of active cell (bottom).

The multiple scale formulation is obtained with a perturbation asymptotic method, described in detail elsewhere [4, 5]. Key assumptions are that velocities are small compared with the speed of sound, and that the flow sweeps a length of the order of the length of the stack. These assumptions lead to a reference Mach number $\mathbf{M} = \frac{L_s}{L_{res}}$. Under these assumptions, the flow in the resonator is characterized by lossless linear acoustics with all dissipation concentrated on the loaded end, and the flow in the active cell is described by nonlinear dynamically incompressible model.
At solid boundaries, continuity of temperature and heat flux and no slip condition are imposed. Temperature $T = T_h$ is fixed on the heater plates, and $T = T_c$ is also fixed on the cooler plates. In the stack plates, the heat conduction equation is solved. The boundaries of the heat exchangers are considered adiabatic.
Matching these two solutions in the standard way provides appropriate boundary conditions to the flow inside the heat exchanger section, depending of the impedance value at the load end. From the standpoint of resonator acoustics, the heat exchanger section is transparent to pressure but provides a source of volume, as a result of the thermoacoustic effect.

2.2 Numerical method

The numerical solution is based upon a finite volume code solving the Navier-Stokes equations under low Mach number assumption [6]. Diffusion is solved implicitly and advection is explicit. Accuracy is second-order in both space and time. In the lossless resonator, acoustics in the two parts can be expressed as two plane waves that move respectively left and right at the speed of sound. At tube ends, using the boundary conditions, the relationship between the incident wave and the reflected wave are expressed as relations between the Riemann invariants, and written on characteristics at the left/right boundaries of the active cell as Riemann invariants considered at previous time. The acoustic pressure does not appear in the active cell, but it modifies these boundaries conditions at each time step.
A Cartesian regular two-dimensional mesh of the active cell is used in the current work (4096× 64 grid points, i.e. 9 grid points across the stack half-plate width, and 37 grid points along the gap between heat exchanger and stack). The numerical calculation is performed

with the following initial condition: a random noise for the velocity field in the whole resonator and a steady state heat conduction condition for the temperature field inside the active cell and constant temperature in the resonator (T_h for the hot part and T_c for the cold part). In order to satisfy a stability criterion (CFL=0.025), the time step must be reduced with the increased horizontal velocity, so that from the initial state to the periodic regime, the whole simulation could be extremely long (about 400 reference acoustic periods), with 200 (initial amplification) to 10000 (periodic regime) time steps per reference acoustic period.

3. Results and discussions

3.1 Reference configuration

Results were obtained for an existing thermoacoustic engine described in [7]. The active cell is inserted in a long resonator tube, closed at both ends. Viscous dissipation inside the resonator plays the role of the load. The experiment uses helium under pressure (p_0), and the cold temperature is considered as the reference temperature, T_c = 293 K. The reference acoustic time (t_{ac}) is approximately equal to 1 ms.
All parameters of the experimental configuration are listed in Table 1. The gap between the stack and the heat exchangers (L_g) was arbitrarily chosen to be equal to twice the plate spacing.

L_{res} (m)	L_s (cm)	H (mm)	L_g (mm)	p_0 (bar)	T_h (K)	t_{ac} (ms)
1	3.5	1.06	1.54	4.4	351.6	1

Table 1: Geometry and condition of experimental device

Analysis of numerical results for initial amplification shows that the load plays an important role to the onset of a thermoacoustic engine. For a given value of a load f, there is a corresponding critical heater temperature, corresponding to each acoustic mode. The limit when f is infinite corresponds to a closed end and the limit when f is zero corresponds to an open end. In order to validate the load model, we identify the load value corresponding to a given experimental setup ($p_0 = 4.4$ bar, $T_h = 662$ K) from the experimental stability curve of the fundamental mode [7]. We obtain a load value of 171.36 $\mathbf{MPa} \cdot \frac{s}{m^3}$. Numerical simulation for this case indicates that the first mode (fundamental) is the most unstable, in agreement with the experiment.
When the heater temperature is further increased for the same mean pressure value, the numerical simulation with the same load value gives the next critical heater temperature $T_h = 820$ K, and both modes 1 and 2 are unstable, again in agreement with experimental results in [7].
In order to study the periodic regime, for a given value of f, we have to choose the heater temperature just above the critical value. By trial and error, we have found that high values of heater temperature (for example $T_h = 743$ K) require long numerical calculation for obtaining a saturated regime. Therefore, the previous load value is not suitable. Numerical experiments showed that, in order to obtain the periodic regime faster we have to choose a higher f. Here for a load of 1523.2 $\mathbf{MPa} \cdot \frac{s}{m^3}$, and the same mean pressure, we obtain the critical heater temperature T_h = 345.7 K. The periodic regime is obtained for $T_h = 351.6$ K. The entire simulation takes about 160 hours CPU time on an INTEL XEON.

3.2 Analysis of periodic regime

In this section, the periodic regime is discussed in detail. All results are presented below using dimensionless values.

Fig. 2 (left) shows the time evolution of the acceleration and the velocity at the left entrance of the simulation domain over one acoustic period. Fig. 2 (right) shows the temperature field over the entire active cell at selected times during the period. Due to the presence of the gap between the heat exchangers and the stack, the temperature gradient along the stack is only 50% of the maximum temperature gradient ($\frac{\Delta T}{L_s}$). The whole acoustic cycle is divided into 21 equal phases. There is interplay between acceleration of the flow and the longitudinal temperature gradient resulting in instability of the Rayleigh-Taylor type. Between the entrance and the exit, the flow has different densities, because of the longitudinal temperature imposed through the heat exchangers. If the hot light fluid is pushing the cool heavy flow, the instability occurs. When the acceleration switches its direction, the flow restabilizes. Here, flow acceleration is directly related to acoustics in the resonators.

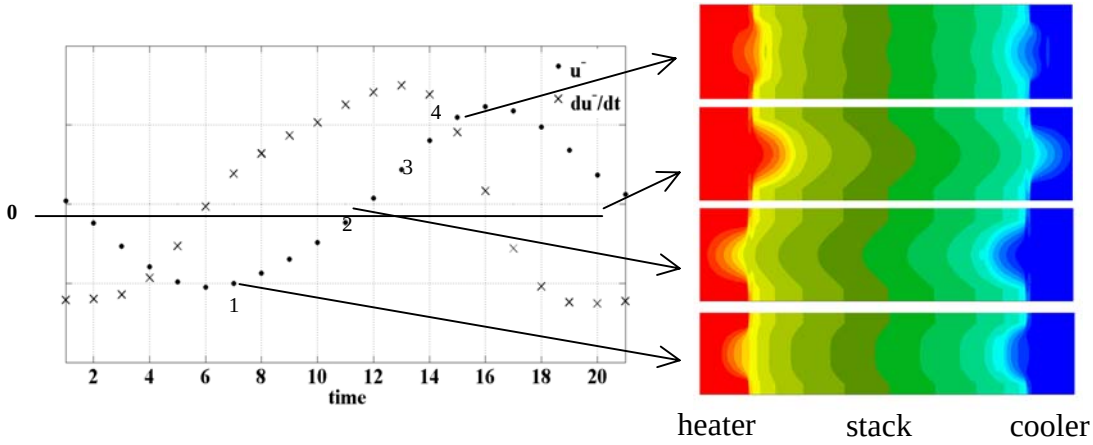

Figure 2: Left: Time evolution of acceleration and velocity at the left entrance of the simulation domain, evolution over one the acoustic period, times 1 to 21. The four points marked on the graph are used in Fig.3. Right: Temperature field over the entire simulation domain at selected times shown by the arrows.

Fig. 3 shows the instantaneous temperature field and the streamlines (left column), and the corresponding vorticity field (right column) between the stack and the heater at 4 different phases of the acoustic cycle (shown in Fig. 2). As expected, one can observe that vortices are generated between the heater and the stack where sudden changes of the cross section exist. Likewise, vortices can be also observed at inlet and outlet of heat exchangers, and between the stack and the cooler (not shown in Fig.3). All vortices are symmetrical in the active cell. From time 1 to time 4, vortices accumulate and roll into the gap between the heater and the stack as long as the flow velocity is significant. Time 1 corresponds to the beginning of flow reversal, and the two vortices grow and move out of the gap. At time 2, vortices move toward the center of the channel. From time 2 to time 3, vortices are sucked outside of the gap area and move toward the right, and recirculation vortices becomes visible in the boundary layer. This continues between time 3 and 4, and finally the plate spacing between two plates of stack can be divided into two boundary layers regions and the domain outside of it. The boundary layer regions absorb the two vortices close to the stack plates, and vortices disappear gradually. A quantitative study of these effects is currently in progress.

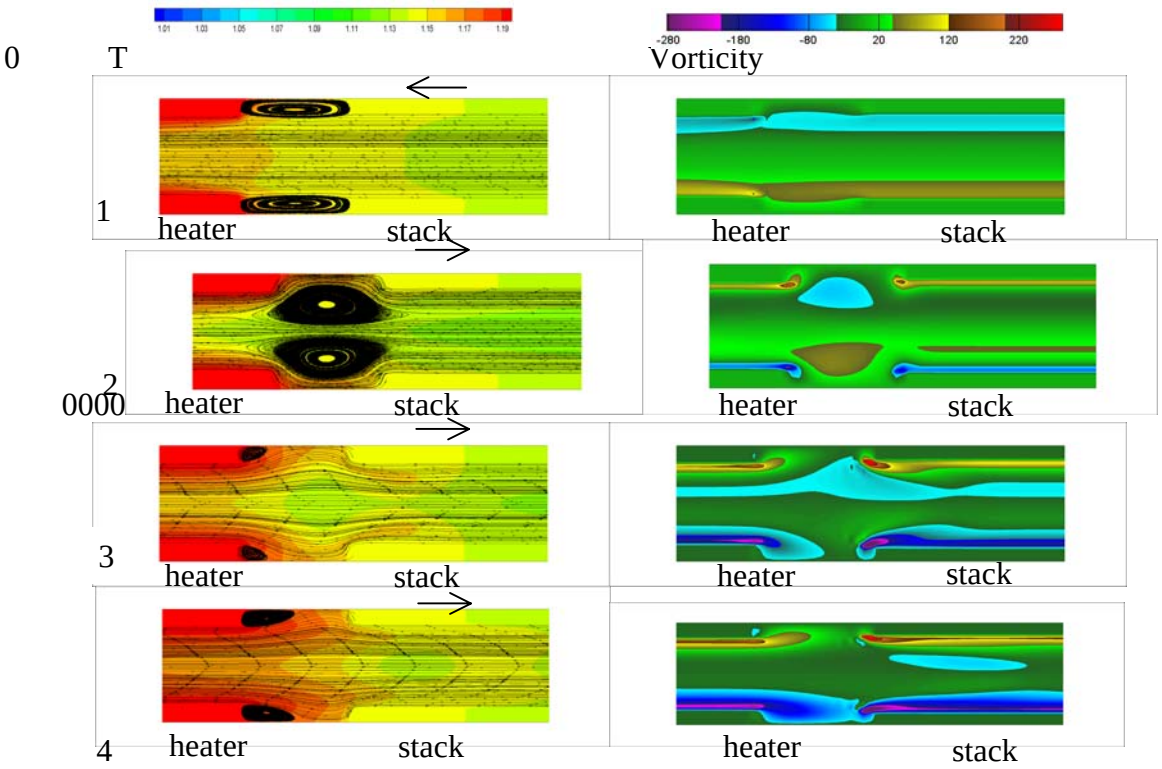

Figure 3: Temperature and streamlines (left) and vorticity fields (right) between the hot heat exchanger and the stack at 4 different time phases (marked on Fig. 2-left).

4. Conclusion

Using a direct simulation, an experimental device of a complete thermoacoustic engine was analysed. In order to obtain the saturation faster, we use a high load value leading to the lower onset temperature. Since due to the temperature difference between the hot and cold heat exchangers, a longitudinal temperature gradient exists, and since both oscillating flow and cross-section changes result in oscillating flow acceleration, the combined effect of the these two features results in a destabilizing/restabilizing mechanism of the Rayleigh-Taylor type. Likewise, the vortex dynamics associated with cavities and step like cross-section changes under oscillating flow show interesting features that are observed in the results, interplaying with temperature gradients and accelerations.

5. References

[1] Rott, N.; Damped and thermally driven acoustic oscillations in wide and narrow tubes. Z. Angew. Math. Phys. 20 (1969) 230-243.
[2] Swift, G.W.; Thermoacoustic engines. J. Acoust. Soc. Am., 84(1988) 1145-1180.
[3] Bauwens, L.; Oscillating flow of a heat-conducting fluid in a narrow tube. J. Fluid. Mech., 324 (1996) 135-161.
[4] Hireche, O.; Weisman, C.; Baltean Carlès, D.; Le Quéré, P.; François, M. X.; Bauwens, L.; Numerical Model of a Thermoacoustic Engine. Comptes rendus Mécanique. 338 (2010) 18-23.
[5] Hireche, O.; Weisman, C.; Baltean Carlès, D.; Le Quéré, P.; Bauwens, L.; Multiple Scale Analysis and Simulation of Thermoacoustic Engines. J. Acoust. Soc. Am.. 128 (2010) 3438-3448.
[6] Le Quéré, P.; Masson, R.; Perrot, P. ; Chebyshev collocation algorithm for 2D non-Boussinesq convection. J. Comp. Physics. 103 (1992) 320-335.
[7] Atchley, A.A; Kuo, F. M.; Stability curves for a thermoacoustic prime mover. J. Acoust. Soc. Am.. 95 (1994) 1401-1404.